

# Colorizing silicon surface with regular nanohole arrays induced by femtosecond laser pulses

Cheng-Yun Zhang,<sup>1,2</sup> Jian-Wu Yao,<sup>1</sup> Hai-Ying Liu,<sup>1</sup> Qiao-Feng Dai,<sup>1</sup> Li-Jun Wu,<sup>1</sup>  
Sheng Lan,<sup>1,\*</sup> Vyacheslav A. Trofimov,<sup>3</sup> and Tatiana M. Lysak<sup>3</sup>

<sup>1</sup>Laboratory of Photonic Information Technology, School of Information and Optoelectronic Science and Engineering, South China Normal University, Guangzhou 510006, China

<sup>2</sup>School of Physics and Electronic Engineering, Guangzhou University, Guangzhou 510006, China

<sup>3</sup>Department of Computational Mathematics and Cybernetics,  
M. V. Lomonosov Moscow State University, Moscow 119992, Russia

\*Corresponding author: slan@scnu.edu.cn

Received October 24, 2011; revised December 16, 2011; accepted January 18, 2012;  
posted January 18, 2012 (Doc. ID 156989); published March 14, 2012

We report on the formation of one- and two-dimensional (1D and 2D) nanohole arrays on the surface of a silicon wafer by scanning with a femtosecond laser with appropriate power and speed. The underlying physical mechanism is revealed by numerical simulation based on the finite-difference time-domain technique. It is found that the length and depth of the initially formed gratings (or ripples) plays a crucial role in the generation of 1D or 2D nanohole arrays. The silicon surface decorated with such nanohole arrays can exhibit vivid structural colors through efficiently diffracting white light. © 2012 Optical Society of America

OCIS codes: 220.4241, 350.3390, 320.7090.

Nanoprocessing technology plays an important role in the fabrication of functional materials and devices. In the last two decades, direct laser writing or ablation has emerged as a fast and efficient technique for fabricating micro- and nanostructures [1,2]. Since the feature size of the fabricated structures is determined by the spot size of the focused laser beam, which is diffraction limited, much effort has been devoted to the study of new mechanisms by which a smaller interaction region or a smaller feature size can be realized [3]. For direct laser writing that has been successfully employed to fabricate three-dimensional (3D) photonic crystals [3,4], a nonlinear process such as two-photon absorption is utilized to reduce the interaction region to a size smaller than the laser spot size [5]. For material processing based on direct laser ablation, on the other hand, various nanostructures with subwavelength feature size induced by pulsed lasers (especially femtosecond [fs] lasers) have received intensive and extensive studies in the last two decades [6]. In practice, periodic micro- and nanostructures are highly desirable, and they are generally produced by using either masks or interfered fs lasers [1,2]. In both cases, however, it is difficult to fabricate nanostructures with subwavelength periods. In addition, these two methods are not suitable for fabricating micro- or nanostructures with a large area. On the other hand, it was discovered a long time ago that ripples with a subwavelength period could be induced on the surfaces of various materials, including metals [7,8], semiconductors [9], and dielectrics [10], when the fluence of the pulsed laser slightly exceeds the ablation threshold. However, the underlying physical mechanism for the formation of such ripples has been debated for a long time [6,11,12]. It is suggested that such ripples may originate from the interference between the surface scattered or excited wave and the laser light itself [11,12].

After the formation of initial ripples, it is expected that the interaction of the laser with the material surface would be changed, leading to the redistribution of the

incident laser that may significantly affect the subsequent ablation process [13]. It has been suggested that the initially formed ripples, which behave as a surface grating, may facilitate the coupling between the incident laser light and the surface plasmon wave [12]. In this case, a further deepening of the ripples is anticipated, resulting in deep grooves on the surface where the incident light is strongly localized. In addition, it has been found that regular surface ripples can be formed by utilizing the interference between the surface plasmon wave generated by gold nanostructures and the incident laser light [14].

In this Letter, we demonstrate numerically and experimentally that regular one-dimensional (1D) nanohole chains and two-dimensional (2D) nanohole arrays can be obtained by deliberately controlling the fluence and scanning speed of a fs laser. We show that long and deep grooves formed on the surface of a silicon wafer will result in the redistribution of the incident laser light inside the grooves, producing 1D and 2D nanohole arrays. A silicon surface decorated with such nanohole arrays exhibits vivid structural colors that span the entire visible spectrum.

In experiments, 1D and 2D nanohole arrays were produced on the surface of a N-doped silicon wafer by using the 800 nm fs laser pulses delivered by a fs amplifier (Legend, Coherent). The duration and repetition rate of the fs laser pulses are 100 fs and 1 kHz, respectively. The resistivity of the silicon wafer is smaller than 0.01  $\Omega$  cm. The surface orientation is (100) and the surface roughness is less than 0.5 nm. The laser beam was focused normally on the surface of the silicon wafer by using a lens with a focusing length of 150 mm, producing a spot of  $\sim 40$   $\mu$ m in diameter. The scanning speed of the laser beam was 1 mm/s, which was found to be an optimum value for the fabrication of regular nanohole arrays. In this case, the average number of fs pulses irradiated on the excitation spot is estimated to be 40.

Figure 1 shows the scanning electron microscopy (SEM) images of the nanostructures induced on the

surface of the silicon wafer that exhibit a strong dependence on the laser fluence ( $F$ ). In our experiments, the polarization and scanning direction of the fs laser were chosen to be the same, as indicated by arrows in the images. For  $F$  smaller than  $103 \text{ mJ/cm}^2$ , no nanostructures were produced. When  $F$  reached  $103.5 \text{ mJ/cm}^2$ , we observed the formation of a 1D nanohole chain, as shown in Fig. 1(a). The nanoholes appeared to be rectangular with a length of  $\sim 0.8 \mu\text{m}$  and a width of  $\sim 0.3 \mu\text{m}$ . The separation between the two neighboring nanoholes was measured to be  $\sim 0.72 \mu\text{m}$ , which was smaller than the laser wavelength. In fact, a close look reveals that the nanoholes in the chain sit on shallow ripples, which can be identified in Fig. 1(a). When  $F$  was increased slightly to  $110 \text{ mJ/cm}^2$ , the nanoholes in the chain became larger and deeper because the incident light was mainly localized in the nanoholes. With a further increase of  $F$  to  $111.4 \text{ mJ/cm}^2$ , we observed a 2D nanohole array composed of two nanohole chains separated by  $\sim 2.0 \mu\text{m}$ , as shown in Fig. 1(b). The number of nanohole chains was increased to three and four when  $F$  was enhanced to  $119.3$  and  $135.3 \text{ mJ/cm}^2$ , respectively [see Figs. 1(c) and 1(d)]. When  $F$  was raised to  $159.2 \text{ mJ/cm}^2$ , we obtained a 2D nanohole array composed of five nanohole chains, as shown in Fig. 1(e). In Fig. 1(f), we show that a 2D nanohole array with two columns of nanoholes can be produced by scanning the laser light with  $F = 111.4 \text{ mJ/cm}^2$  vertically. This indicated that the formation and arrangement of nanohole arrays are strongly related to the polarization of laser light.

In order to find out the physical origin for the formation of 1D and 2D nanohole arrays, we have calculated by numerical simulation the electric field distribution on a

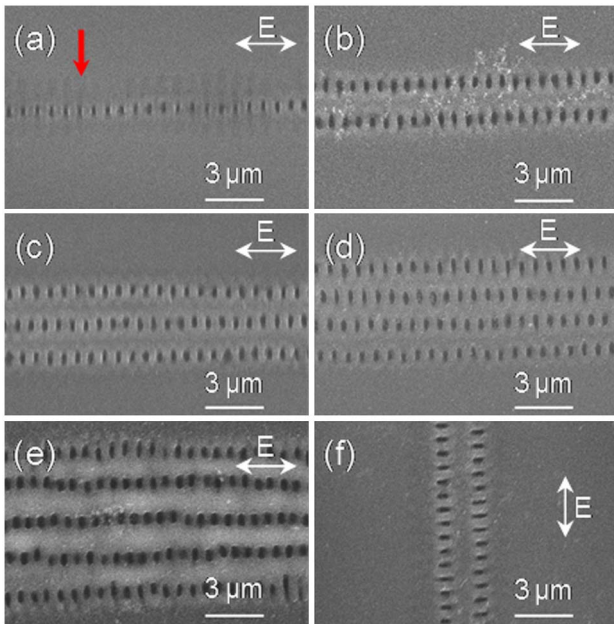


**Fig. 1.** (Color online) 1D and 2D nanoholes arrays induced on the surface of a silicon wafer by scanning a fs laser with a speed of  $1 \text{ mm/s}$  and different fluences ( $F$ ): (a)  $F = 103.5 \text{ mJ/cm}^2$ , (b)  $F = 111.4 \text{ mJ/cm}^2$ , (c)  $F = 119.3 \text{ mJ/cm}^2$ , (d)  $F = 135.3 \text{ mJ/cm}^2$ , (e)  $F = 159.2 \text{ mJ/cm}^2$ , (f)  $F = 111.4 \text{ mJ/cm}^2$ . In each case, the laser polarization is indicated by an arrow and the scanning direction was chosen to be parallel to the laser polarization.

grooved surface (i.e., the surface with periodic ripples) by using the finite-difference time-domain (FDTD) technique [15]. The simplified physical model used in the numerical simulations is schematically shown in Fig. 2(a). It is assumed that five grooves have been produced on the surface of the silicon wafer along the  $y$  axis as a result of ripple formation. The geometry of the grooves can be described by four parameters  $l$ ,  $w$ ,  $h$ , and  $d$ , which denote the length, width, depth, and period of the grooves, as depicted in Fig. 2(a). In the normal state, the extinction coefficient of silicon is found to be  $\kappa = 0.04$  at  $800 \text{ nm}$  [16]. Under the irradiation of fs laser pulses, however, the complex refractive index of silicon would be dramatically modified due to the high density of photogenerated carriers [12,17]. The dependence of the complex refractive index of silicon on carrier density has been calculated previously [17]. Since the laser fluences we used were just above the damage threshold of silicon, the real part of the refractive index remained nearly unchanged while a significant increase in  $\kappa$  was expected. Therefore, the complex refractive index of silicon was chosen to be  $n = 3.4 + i0.5$  in the numerical simulations [17]. It was revealed that the large  $\kappa$  of silicon induced by fs laser irradiation played a crucial role in localizing laser light in the grooves. In the numerical simulations, the laser beam polarized along the  $x$  axis was normally incident on the silicon wafer, and the electric field ( $E_x$ ) distribution on the surfaces of the grooves was recorded by field detectors. The diameter of the laser beam was assumed to be much larger than the area with grooves. Based on experimental observations, we fixed  $w$  and  $d$  to be  $0.3$  and  $0.8 \mu\text{m}$  and varied  $l$  and  $h$  to see the change in the electric field distribution. Some typical results are shown in Figs. 2(b)–2(f).

For short and shallow grooves with  $l < 4.0 \mu\text{m}$  and  $h < 0.10 \mu\text{m}$ , numerical simulation indicated that the electric field was concentrated at the center of each groove, as shown in Fig. 2(b). It implied that the subsequent ablation occurred preferentially at the center

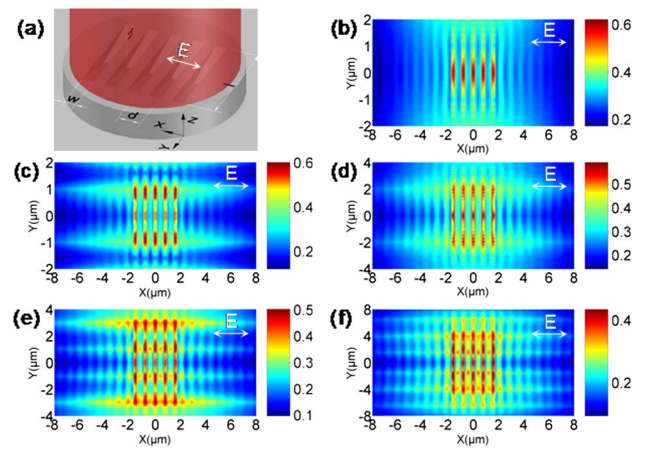


**Fig. 2.** (Color online) Schematic showing the geometry of the initially formed grooves (ripples) on the surface of the silicon wafer that was employed in numerical simulation (a) and the calculated electric field distributions on the surface of grooves whose structural parameters are chosen to be (b)  $l = 4.0 \mu\text{m}$ ,  $h = 0.06 \mu\text{m}$ ; (c)  $l = 4.0 \mu\text{m}$ ,  $h = 0.12 \mu\text{m}$ ; (d)  $l = 8.0 \mu\text{m}$ ,  $h = 0.10 \mu\text{m}$ ; (e)  $l = 8.0 \mu\text{m}$ ,  $h = 0.16 \mu\text{m}$ ; (f)  $l = 16 \mu\text{m}$ ,  $h = 0.18 \mu\text{m}$ .

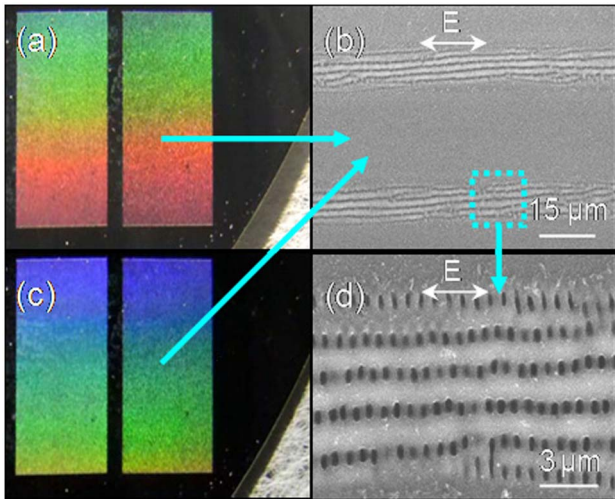


Fig. 3. (Color online) (a), (c) Surface colors observed by shining a white light on the surface of the silicon with different incidence angles. The SEM images for the processed silicon surface are presented in (b) and (d). The 2D nanohole array was fabricated with a laser fluence of  $159.2 \text{ mJ/cm}^2$ , a scanning speed of  $1 \text{ mm/s}$ , and an interspace of  $30 \mu\text{m}$ .

of each groove, leading to the formation of a 1D nanohole chain. For larger laser fluences, it was expected that deeper and longer grooves would be created on the surface. In this case, the number of the maximums in the electric field distribution increased with increasing length and depth of the grooves. In Fig. 2(c), two maximums can be clearly identified in the electric field distribution for each groove. It implies that a 2D nanohole array composed of two nanohole chains will be achieved. In Figs. 2(d)–2(f), we present the numerical simulation results for the electric field distributions in longer and deeper grooves. Three, four, and five maximums, which are symmetrically distributed on the two sides of the central line, are found to appear in the electric field distribution for each groove. Consequently, the ablation takes place preferentially at these points, resulting in 2D nanohole arrays. These results indicate that the number of nanoholes (i.e., the number of maximums in the electric field distribution) formed in each groove depends strongly on the length and depth of the grooves that is determined by laser fluence. Since the formation of the grooves and their geometries are crucial for the creation of regular nanohole arrays, the scanning speed of the laser beam should be optimized and the laser fluence must be carefully adjusted.

Previously, the surface ripples induced by fs laser pulses on silicon have been employed to realize an anti-reflection effect over a wide wavelength range [18]. By scanning the laser beam line by line on the surface of the silicon wafer with appropriate power and speed, we can easily obtain 2D nanohole arrays with different area densities. A silicon surface decorated with high-density nanoholes can be achieved by using a laser fluence of  $159.2 \text{ mJ/cm}^2$  and an interspace of  $30 \mu\text{m}$ , as shown in Fig. 3. The 2D nanohole arrays fabricated on the surface

of the silicon wafer possessed uniform size and period. It is manifested in the fact that the processed surface can efficiently diffract white light and give rise to vivid structural colors. As shown in Figs. 3(a) and 3(c), one can see different structural colors emerging from the surface, which is irradiated with white light. Red, green, and blue colors appear at different places of the surface because of the different incidence angles.

In summary, we have demonstrated the formation of 1D and 2D nanohole arrays on the surface of a silicon wafer by scanning a fs laser with optimized energy density and speed. We illustrated the underlying physical mechanism by numerical simulation based on the FDTD technique. It was found that the length and depth of initially formed grooves are crucial for the generation of nanohole arrays. The surfaces decorated with such nanohole arrays exhibit efficient diffraction for white light. This technique may be developed for applications in the fields of anti-counterfeiting, color display, decoration, encryption, and optical data storage.

The authors acknowledge financial support from the National Natural Science Foundation of China (Grant Nos. 10974060, 51171066, and 1111120068) and the project for high-level professionals in the universities of Guangdong Province, China.

#### References and Notes

1. M. Y. Shen, C. H. Crouch, J. E. Carey, R. Younkin, E. Mazur, M. Sheehy, and C. M. Friend, *Appl. Phys. Lett.* **82**, 1715 (2003).
2. Y. Nakata, T. Okada, and M. Maeda, *Appl. Phys. Lett.* **81**, 4239 (2002).
3. R. R. Gattass and E. Mazur, *Nat. Photon.* **2**, 219 (2008).
4. T. Kondo, S. Matsuo, S. Juodkazis, and H. Misawa, *Appl. Phys. Lett.* **79**, 725 (2001).
5. S. Kawata, H. B. Sun, T. Tanaka, and K. Takada, *Nature* **412**, 697 (2001).
6. P. Schaaf, ed., *Laser Processing of Materials: Fundamentals, Applications and Developments* (Springer, 2010).
7. A. Y. Vorobyev and C. Guo, *Appl. Phys. Lett.* **92**, 041914 (2008).
8. A. Y. Vorobyev and C. Guo, *J. Appl. Phys.* **103**, 043513 (2008).
9. A. Y. Vorobyev and C. Guo, *Opt. Express* **18**, 6455 (2010).
10. Q. Zhang, H. Lin, B. Jia, L. Xu, and M. Gu, *Opt. Express* **18**, 6885 (2010).
11. J. E. Sipe, J. F. Young, J. S. Preston, and H. M. van Driel, *Phys. Rev. B* **27**, 1141 (1983).
12. M. Huang, F. L. Zhao, Y. Cheng, N. S. Xu, and Z. Z. Xu, *ACS Nano* **3**, 4062 (2009).
13. G. Obara, N. Maeda, T. Miyanishi, M. Terakawa, N. N. Nedyalkov, and M. Obara, *Opt. Express* **19**, 19093 (2011).
14. G. Obara, Y. Tanaka, N. N. Nedyalkov, M. Terakawa, and M. Obara, *Appl. Phys. Lett.* **99**, 061106 (2011).
15. A commercially available software developed by RSoft Design Group (<http://www.rsoftdesign.com>) is used for the numerical simulations.
16. D. E. Apens, *Properties of Silicon* (INSPEC, IEE, 1988).
17. J. Bonse, A. Rosenfeld, and J. Krüger, *Appl. Surf. Sci.* **257**, 5420 (2011).
18. A. Y. Vorobyev and C. Guo, *Opt. Express* **19**, A1031 (2011).